

Advanced oxidation processes for waste water treatment: from laboratory-scale model water to on-site real waste water

Julien G. Mahy , Cédric Wolfs , Christelle Vreuls , Stéphane Drot , Sophia Dircks , Andrea Boergers , Jochen Tuerk , Sophie Hermans & Stéphanie D. Lambert

To cite this article: Julien G. Mahy , Cédric Wolfs , Christelle Vreuls , Stéphane Drot , Sophia Dircks , Andrea Boergers , Jochen Tuerk , Sophie Hermans & Stéphanie D. Lambert (2020): Advanced oxidation processes for waste water treatment: from laboratory-scale model water to on-site real waste water, Environmental Technology, DOI: [10.1080/09593330.2020.1797894](https://doi.org/10.1080/09593330.2020.1797894)

To link to this article: <https://doi.org/10.1080/09593330.2020.1797894>

 [View supplementary material](#) 

 Published online: 28 Jul 2020.

 [Submit your article to this journal](#) 

 Article views: 111

 [View related articles](#) 

 [View Crossmark data](#) 



Advanced oxidation processes for waste water treatment: from laboratory-scale model water to on-site real waste water

Julien G. Mahy ^{a,b,d}, Cédric Wolfs^a, Christelle Vreuls^c, Stéphane Drot^c, Sophia Dircks^d, Andrea Boergers^d, Jochen Tuerk^d, Sophie Hermans ^b and Stéphanie D. Lambert^a

^aDepartment of Chemical Engineering – Nanomaterials, Catalysis & Electrochemistry, University of Liège, Liège, Belgium; ^bInstitute of Condensed Matter and Nanosciences (IMCN), Université catholique de Louvain, Louvain-la-Neuve, Belgium; ^cEnvironmental Department, Celabor, Research Centre, Herve, Belgium; ^dInstitut für Energie- und Umwelttechnik e.V. (IUTA, Institute of Energy- and Environmental Technology), Duisburg, Germany

ABSTRACT

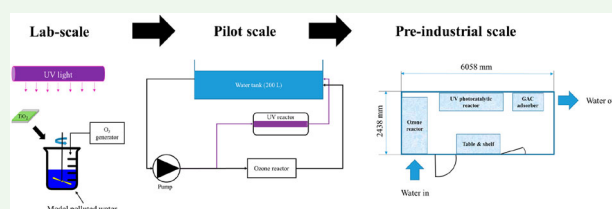
A process combining three steps has been developed as a tertiary treatment for waste water in order to remove micropollutants not eliminated by a conventional waste water treatment plant (WWTP). These three processes are ozonation, photocatalysis and granulated activated carbon adsorption. This process has been developed through three scales: laboratory, pilot and pre-industrial scale. At each scale, its efficiency has been assessed on different waste waters: laboratory-made water, industrial waste water (one from a company cleaning textiles and another from a company preparing culture media, both being in continuous production mode) and municipal waste water. At laboratory scale, a TiO₂-based photocatalytic coating has been produced and the combination of ozonation-UVC photocatalytic treatment has been evaluated on the laboratory-made water containing 22 micropollutants. The results showed an efficient activity leading to complete or partial degradation of all compounds and an effective carbon for residual micropollutant adsorption was highlighted. Experiments at pilot scale (100 L of water treated at 500 L/h from a tank of 200 L) corroborated the results obtained at laboratory scale. Moreover, tests on municipal waste water showed a decrease in toxicity, measured on *Daphnia Magma*, and a decrease in micropollutant concentration after treatment. Finally, a pre-industrial container was built and evaluated as a tertiary treatment at the WWTP Duisburg-Vierlinden. It is shown that the main parameters for the efficiency of the process are the flow rate and the light intensity. The photocatalyst plays a role by degrading the more resistant micropollutants. Adsorption permits an overall elimination >95% of all molecules detected.

ARTICLE HISTORY

Received 14 November 2019
Accepted 25 May 2020

KEYWORDS

Micropollutant elimination; waste water treatment; UVC photocatalysis; ozonation; granulated activated carbon adsorption



1. Introduction

For decades, environmental issues have been in the centre of attention concerning the production of greenhouse gases, deforestation or pollution of air, soil and water. Indeed, degradation of the environment quality can cause serious damages to human health, fauna and flora [1]. In particular, water pollution can lead to eutrophication of lakes or rivers, development of illnesses such as cancer and hormonal imbalance. The pollutants can be heavy metals, pesticides, pharmaceutical products, chlorinated compounds or other organic

compounds [1]. For a few years, micropollutants have been attracting considerable attention [2–4]. Indeed, these compounds are present only in trace amounts at the exit of conventional waste water treatment plants. Even if these micropollutants represent very low quantities, a long-term exposure to this pollution can have negative consequences.

The European Union has started to list some priority micropollutants in its water framework directive (WFD) [5]. For now, research focuses on the development of efficient processes for micropollutant elimination [6,7].

CONTACT Julien G. Mahy  julien.mahy@ulclouvain.be  Institute of Condensed Matter and Nanosciences (IMCN), Université catholique de Louvain, Place Louis Pasteur 1, Louvain-la-Neuve 1348, Belgium

 Supplemental data for this article can be accessed <https://doi.org/10.1080/09593330.2020.1797894>.

© 2020 Informa UK Limited, trading as Taylor & Francis Group

Among these processes, advanced oxidative processes (AOP) represent a potential way to degrade a large range of organic micropollutants. These AOPs can be ozone oxidation [6,8], titania-based photocatalytic processes [9–11] or (photo)-Fenton reactions [12,13]. They require the production of radicals, especially the hydroxyl radical (OH \cdot), to oxidize and degrade these organic substances.

Many studies showed the efficiency of AOPs for organic pollutant elimination. For example, Lopez-Vinent *et al.* [14] showed the efficiency of a photo-Fenton process using UV-A LEDs for the degradation of diphenhydramine hydrochloride after only 1 h. In Yang *et al.* [15], graphitic carbon nitride modified TiO $_2$ combined with persulfate was able to remove bisphenol A in only 15 min. This system was also efficient on the degradation of caffeine, phenol and acetaminophen. In Wardenier *et al.* [16], different AOPs, such as O $_3$, UV or plasma-ozonation, were evaluated on a model water composed of 4 micropollutants (atrazine, alachlor, bisphenol A and 1,7- α -ethinylestradiol) at concentration 1 mg/L each. Plasma-ozonation showed the fastest elimination rate, degrading more than 95% of the pollutants in only 20 min despite a high energy cost. In Seo *et al.* [17], an UV/H $_2$ O $_2$ process was tested on real waste water at laboratory scale showing its efficiency regarding micropollutant elimination (phenolic and olefinic moieties). The review of Miklos *et al.* [18] detailed the different AOPs studied in the literature, and links different parameters (nature of the process, scale, type of water etc.) to the median energy consumption of these processes. In this review, UV/O $_3$ processes lie among the realistic candidates for full-scale applications, whereas photocatalysis is considered much less efficient.

Nevertheless, the large majority of published works concerns laboratory-scale studies on model water.

In this work, a tertiary waste water treatment was developed and evaluated through laboratory scale, pilot scale and pre-industrial scale. This process combines an ozonation step, a UVC-photocatalytic step and a granulated active carbon (GAC) adsorption step. At laboratory scale, an efficient TiO $_2$ -based coating was developed and assessed on water containing 22 micropollutants. The details of this development were published in [5]. In this work, deposition of titania at pilot and pre-industrial scale was done with spray coating. The efficiency of the pilot reactor was assessed on laboratory-made water, real waste water from industrial plants and municipal waste water. Besides this pilot reactor, a pre-industrial set-up was also tested on up to 5 m 3 /h of waste water originating from the treatment plant.

2. Materials and methods

2.1. Photocatalyst synthesis

The photocatalyst is a TiO $_2$ material doped with 2 wt.% of silver mixed with 10 wt.% of commercial Evonik P25, what we named Ag2/10P25. The synthesis is detailed in [5]. The composition of the TiO $_2$ coating is based on our previous study [5] for the removal of micropollutants. The role of P25 is to increase the roughness of the coating which leads to better activity via an increase of the specific surface of the layer. Using silver also increases the degradation efficiency by its role of electrons trap. Moreover, silver has also anti-microbial properties which could have a biological role on the contaminants. The composition was optimized in [5].

First, silver acetate (Merck, purity \geq 99%, called AgAc) was stirred in 2-methoxyethanol (Acros Organics, purity \geq 99.5%, called MetOH). Then, *N*-[3-(trimethoxysilyl)propyl]ethylenediamine (Sigma-Aldrich, purity 97%, called EDAS) was added to the solution. Pre-hydrolysis of EDAS was made by adding ultrapure water (18.2 M Ω -cm $^{-1}$) to the solution.

In another container, titanium tetraisopropoxide (Sigma-Aldrich, purity \geq 97%, called TTIP) was dissolved in MetOH. Evonik P25 particles were added to this solution, which was then heated to 80°C under stirring. Twelve hours later, the P25+TTIP solution was sonicated by ultrasound (Branson 2510 ultrasonicator) for 15 min. Then, the sonicated solution was added to the main solution. The solution was put under a nitrogen atmosphere. Ultrapure water was mixed with the solution.

The weights and volumes of the reagents are shown in Table S1 in Supplementary Materials.

2.2. Laboratory scale

2.2.1. Coating

The TiO $_2$ photocatalyst is deposited on stainless steel slides (316L steel, Mecanic Systems, Braine-l'Alleud, Belgium) of dimension 25 mm \times 75 mm \times 0.7 mm.

The slides were washed, dipped in a 2 mol/L solution of HNO $_3$ for 5 s and dried. Then, they were manually spray-coated using an airbrush (Harder & Steenbeck) with the nozzle at about 5 cm above the slide and using 3-bar compressed air for spraying. The amount of TiO $_2$ solution sprayed was 2 mL with a flow of 0.13 mL/min. Afterwards, the slides were calcined at 390°C for 12 h.

The coating crystallinity was characterized by grazing incidence X-ray diffraction (GIXRD) in a Bruker D8 diffractometer (Bruker, Billerica, MA, USA) using Cu-K α radiation and operating at 40 kV and 40 mA. The incident beam angle was 0.5°.

A corresponding powder sample (i.e. powder made from the same sol as the studied layer) was studied using transmission electron microscopy (TEM-Philips CM-100 operating at 130 kV) as well as scanning transmission electron microscopy (STEM) coupled with energy-dispersive X-ray (EDX) to confirm the presence of silver.

Titania coatings were also investigated using a JEOL JSM-840 (JEOL, Peabody, MA, USA) scanning electronic microscope (SEM) at an acceleration voltage of 20 kV. An elemental analysis by energy-dispersive X-ray spectroscopy (EDX) was also performed.

2.2.2. Degradation test on the model water

The model water is composed of 22 micropollutants with a concentration of 10 µg/L for each one. The micropollutants were lindane, atrazine, 2,2',4,4',6-penta-bromodiphenyl ether, tributylphosphate, di(2-ethylhexyl)phthalate, metoprolol, carbamazepine, diclofenac, sulfamethoxazole, 1H-benzotriazole, desethylatrazine, 2,6-dichlorobenzamide, bromacil, simazine, chlortoluron, isoproturon, dichlorodiphenyltrichloroethane (DDT), acetyl-4-sulfamethoxazole, iohexole, iopromide, clarithromycin and terbutryn.

Using EU's Water Framework Directive (Directive 2000/60/EC) as a starting point, the identification of relevant micropollutants was focused on 'priority pollutants', such as pesticides, industrial chemicals, pharmaceuticals and personal care products (PCP). Each of the chosen micropollutants appears clearly in that directive. The most common medicines and pesticides in Belgium and Germany were focused on, in order to facilitate the study of real waste water.

The degradation experiment is fully detailed in [5] and detailed in the following paragraphs.

2.2.2.1. Degradation experiment protocol. The testing protocol was as follows:

- i 420 mL of a solution containing all 22 pollutants was poured into a stirred glass bottle. The first sample of 60 mL was immediately taken to measure the initial concentration of the 22 pollutants [5].
- ii The glass bottle was wrapped in an aluminium foil in order to protect the solution from light. An Aqua Medic Ozone 200 device was used for the ozonation (ozone was injected by a diffuser), which produces 200 mg O₃/h. The solution was ozonated for 30 min (with a concentration of 15 mg/L in the solution measured with the Ozone MColorstest Disk comparator test from VWR). The second sample of 60 mL was then taken [5].

- iii The solution was transferred into a crystallizing bowl with four coated slides. The bowl was covered by a quartz plate, which was transparent to UVC radiation. It was stirred by an orbital shaker (Grant Bio POS 300) throughout the rest of the experiment. The system was placed inside a thermostatic box at 15°C in the dark for 30 min. After that, the third sample of 60 mL was taken [5].
- iv The UVC lamp ($\lambda = 254$ nm, 20 W/m² at the photocatalyst surface) was turned on. After different times (1, 2, 4, 6 h), a sample of 60 mL was taken (from the total of 240 mL at the end of (iii)) and one of the four slides was removed, in order to keep the concentration of photocatalyst constant in the solution until the end of the photocatalytic test [5].

In addition, one experiment was conducted without any slides, but with an otherwise identical protocol. Measurements of the degradation of the 22 pollutants by ozone and UVC alone were made possible by this 'blank experiment' [5].

Finally, another experiment was carried out in the presence of the slides but without light. This was done in order to evaluate the adsorption of the micropollutants onto the slides (dark experiment) [5].

For the laboratory scale, the concentration of catalyst was 2.5×10^{-2} m² of catalyst/L.

Each sample was analyzed using GC/MS-MS and LC/MS-MS. Detailed information about the chromatography is given in the next sections.

2.2.2.2. GC-MS method. A stock solution of all the micropollutants was prepared at 1000 ppm in methanol and stored at -20°C. Ultrasonication was used to improve solubility. A calibration curve was constructed from 0.01 ppm to 5 ppm for the GC/MS-MS technique [5].

To quantify phthalates and prevent contamination, plastic containers could not be used. All glass apparatus was rinsed with acetone and then with hexane Pestican®. Nitrile gloves had to be used [5].

The decantation took place in a separatory funnel of 100 ml under agitation for 1 h. About 50 mL of sample was mixed with 5 g of MgSO₄ and 20 mL of a 90/10 mixture of hexane/acetate ethyl. The aqueous phase was collected and a second extraction was performed for 1 h with 20 mL of a mixture of 50/50 hexane/acetate ethyl. The organic phase was filtered on anhydrous Na₂SO₄ and evaporated until 0.5 mL remained. 1.5 mL of hexane was added and samples were separated into 2 vials for GC-MS injection [5].

The XLB-type chromatography column, a Trace GC Ultra system from Thermo Scientific (Thermo Fisher Scientific, Waltham, MA, USA), was of dimensions

30 m × 0.25 mm × 0.25 μm. Helium was used as a carrier gas and the temperature gradient could reach 320°C [5].

The retention times of the different micropollutants are described in Table S2. The chromatogram (see Figure S2 from [5]) highlights that the different compounds are well separated in terms of retention time. Simazine and atrazine were co-eluted but had different daughter ions to differentiate them [5].

The substances were analyzed with an ITQ Series GC/MS Ion Trap Mass Spectrometer from Thermo Scientific [5].

2.2.2.3. LC-MS/MS method. Methods were first developed for the quantification of the model water composed of 5 micropollutants [5]. Afterwards, the quantification method was adapted for the extended model water containing 10 micropollutants [5]. More information about the LC-MS/MS measurement method is shown in Table S3.

The chromatogram from Figure S3 in [5] shows the detection peaks of almost all substances of the extended micropollutant list. For all substances, it can be seen that the substance peaks are well separated [5].

The substances described were measured with an Agilent 1100 LC system (Agilent Technologies Deutschland GmbH, Germany) coupled to a Sciex QTRAP 6500 mass spectrometer (AB Sciex Germany GmbH, Germany) according ISO 21676 (2018). For separation, a Raptor ARC-18 (Resteck GmbH, Germany) column was used. LC-MS-grade water (A) and acetonitrile (B), each with 0.1% formic acid, were used as solvents. The gradient of the solvents is shown in Table S4 [5].

For calibration, an intermediate dilution was prepared from the stock solution. The stock solution was prepared at 1 g/L in 50% acetonitrile and 50% LC-MS water and stored below 8°C. Each calibration had to be prepared daily for each sample series. It was calibrated in the range of 0.001–100 ng/mL.

2.2.3. Adsorption step

As the last step of the whole process at large scale will be an adsorption on GAC, adsorption experiments were conducted at laboratory scale to find an efficient and low-cost commercial GAC material adapted for micropollutant adsorption.

Seven different activated carbons were chosen (Table 1) for laboratory-scale selection. They were chosen among three different suppliers and covered their full price range (~1880–2700 €/ton), in order to check if the price was correlated with adsorption capacities. Their specific surface area (S_{BET}) was determined thanks to nitrogen adsorption–desorption isotherms measured

with an ASAP 2420 multi-sampler adsorption–desorption volumetric device from Micromeritics.

The carbons were ground to particulate activated carbon (PAC) and sieved. PACs with a particle size smaller than 50 μm were used to produce a carbon suspension of 10 mg/L. Each PAC was put in contact with water containing a certain type of micropollutant (metoprolol or 1H-benzotriazole, 10 μg/L). These samples were stirred for 120 min on a shaker rotating at 200 rpm. After 0, 5, 15, 30, 60 and 120 min, the samples were filtered with a syringe filter of 0.45 μm and analyzed via LC-MS/MS to follow the micropollutant concentration.

2.3. Pilot scale

2.3.1. Coating

The pilot-scale reactor being a cylindrical steel reactor (picture in [5]), the coating needed to be done on the inside surface. An industrial spray-coater (Aquatic Science S.A.A, Herstal, Belgium) was used for deposition. A nozzle moving vertically along the central axis of the reactor from the top allowed the deposition. First, a nitric acid solution (weight concentration 50%) was abundantly sprayed inside the reactor, which was then dried at 120°C [5]. 7 mL of a freshly prepared TiO₂ sol was sprayed on the dry inner surface, and the reactor was dried at 120°C again, before being calcined at 390°C for 12 h [5].

2.3.2. Pilot scale degradation experiments on model water and real waters

The pilot set-up was shown in [5]. It is composed of a tank (200 L), an ozonation reactor (O₃ generation of 60 g/h, ozone was injected by a Venturi injector) and a photocatalytic reactor (UVC 254 nm monochromatic lamp, 110 W/m² at the interior surface). The polluted water circulated continuously at a flowrate of 500 L/h. Sampling was done after 30 min of ozonation (with an ozone concentration of 0.42 mg/L at permanent

Table 1. Carbon properties.

Carbon	Notation	Cost [19–21] (€/ton)	S_{BET} (m ² /g)
Donau Carbon Hydriffin 30N	DC 30N	1880	1035
Donau Carbon Hydriffin CX 30	DC CX30	2300	916
Donau Carbon Hydriffin A 8x30	DC A	2700	1159
Donau Carbon Hydriffin CC 8x30 plus	DC CC plus	3895	1240
CSC GAK 1	GAK 1	2265	943
CSC GAK 2	GAK 2	2165	981
CarboTech DGF 8x30	DGF	1410	1060
	Carbotech		

S_{BET} : specific surface area estimated by the Brunauer, Emmett, Teller (BET) method [22].

regime), and after a further 1 h of photocatalysis. The concentration of catalyst was $1.36 \times 10^{-3} \text{ m}^2$ of catalyst/L. The experiments were repeated with an uncoated reactor in order to check the efficiency of the photocatalyst layer.

Different polluted waters were tested: the laboratory-made water containing 22 micropollutants; two types of industrial waste water (one from a company cleaning textiles containing biocides, the other from a company preparing culture media); and finally, the outlet of a municipal waste water treatment plant (Esneux WWTP, Belgium).

The water parameters denoted in Table 2 were measured before applying the AOP process.

In the case of laboratory-made water, the pollutant concentrations were evaluated with GC-MS and LC-MS/MS. As for the two types of industrial waste water, only the toxicity before and after treatment was evaluated. The toxicity test is based on the ISO 6341 standard [23]. During this experiment, *Daphnia magna* microcrustaceans were incubated for 24 h in the toxic water at different concentrations [5]. After 24 h of contact, the number of immobile microcrustaceans was counted [5]. This number was plotted against the concentration of the toxic water. From this, the relative concentration EC50, at which half of the microcrustaceans died, was found [5]. EC50 is expressed in the per cent of the initial concentration of the toxic water. The toxicity unit (TU) of the water is defined as $TU = 100\%/EC50$. The water was considered toxic if $1 < TU < 10$, and very toxic if $TU > 10$ [5].

The toxicity test was also performed on the municipal waste water, and the micropollutant content before and after treatment was assessed with LC-MS/MS.

2.4. Pre-industrial scale

2.4.1. Container building

The pre-industrial test was conducted on the installation represented as Figure 1. 40 g/h of ozone was produced locally from an electric discharge in the presence of oxygen, so that the ozone concentration at permanent regime was equal to around 5 mg/L. The water is then sent to the UV reactor. The UV reactor is equipped with

a light sensor, able to measure the energy at the inner surface of the reactor, as well as a pH electrode. The water flows out into a cylindrical GAC adsorber of height 2.5 m and of diameter 1.2 m. This adsorber can be filled with up to 700 kg of the chosen carbon (*i.e.* Carbotech DGF 8×30 GL). Between the UV-system and the adsorber, the flowrate is measured, and samples can also be taken for analysis.

The full process can be transported in a standard 10 ft container (length 6.06 m, width 2.44 m, height 2.6 m). This ease of transportation will facilitate future research on the subject, since the location of the system, and thus the composition of the inlet waste water, can be changed readily. As indicated on the diagram, a work bench is also installed for operation and maintenance of the equipment.

2.4.2. Coating

Two pre-industrial scale reactors were coated in the same manner as the pilot scale reactor. These reactors are cylindrical, and are of resp. diameter and length $20 \times 90 \text{ cm}$ (the catalyst surface area was equal to 0.565 m^2) and $40 \times 90 \text{ cm}$ (the catalyst surface area was equal to 1.131 m^2). Again, a nozzle moved vertically along the central axis of the reactors. First, a nitric acid solution (weight concentration 50%) was abundantly sprayed inside each reactor, which was then dried. Then, 20 mL of a freshly prepared TiO_2 sol was sprayed onto the inner surface of each reactor. Both reactors were calcined at 550°C for 2 h.

2.4.3. Degradation experiments on the waste water treatment plant

Degradation experiments were carried out using water at the outlet of Duisburg's Waste Water Treatment Plant in Germany.

Depending on the experiment, several combinations were tested, amongst the following parameters:

- i type of lamp: either medium pressure (power 7 kW) or low pressure (power 200 W), emitting monochromatic light (wavelength 254 nm);
- ii choice of reactor: one of those described in 2.4.2;
- iii coating: either present or absent;
- iv waste water flow rate: anywhere between 0 and $5 \text{ m}^3/\text{h}$.

For each experiment, micropollutant concentrations were assessed with LC-MS/MS methods similarly to the laboratory experiments (LC-MS/MS methods are detailed in Supplementary Materials)

Table 2. Characteristic waste water parameters before the pilot scale experiments.

Waste water	COD (mg O ₂ /L)	N _{total} (mg/L)	P _{total} (mg/L)
Textile water	1416	14.5	2.1
Culture media water	500	20.0	2.0
Municipal water	83	11.6	1.8

COD: chemical oxygen demand; N_{total}: total nitrogen amount; P_{total}: total phosphorus amount.

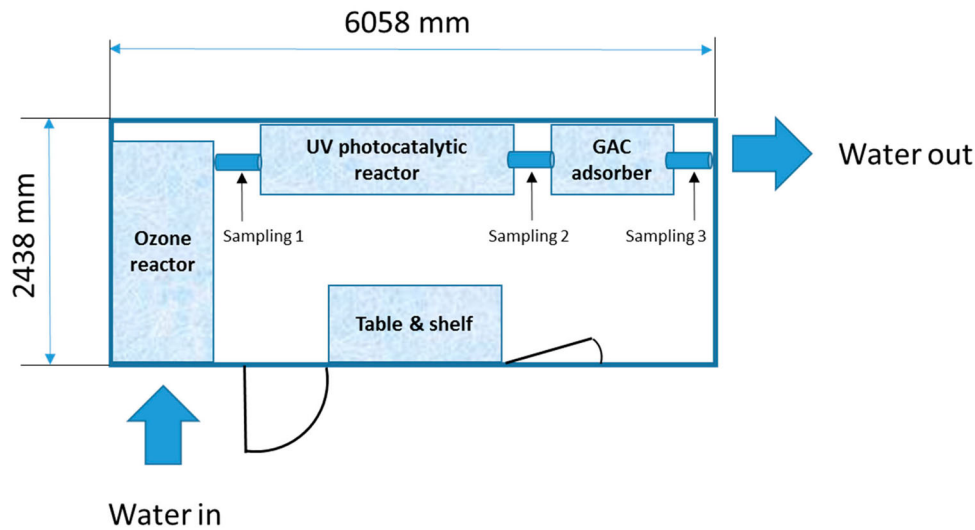


Figure 1. Pre-industrial installation scheme.

3. Results and discussion

3.1. Laboratory scale

3.1.1. TiO_2 coating

The crystallinity of the TiO_2 coating deposited on steel slides at laboratory scale was observed with GIXRD, as shown by the pattern represented in [Figure 2](#). Three peaks are observed: one at 25° corresponding to the TiO_2 anatase phase of the coating, and two at 43.5° and 50.7° , corresponding to chromium iron carbide from the steel substrate. The silver present in the coating was not detected with GIXRD as the amount is very low (2 wt. %) [[5,24](#)] and the crystallites supposedly

very small (around 3 nm as described in [[2,5,24,25](#)]). Evonik P25, which is TiO_2 composed of anatase (80%) and rutile (20%) [[26,27](#)], was also not seen as such. Indeed, the amount of rutile is also too low to be detected [[5](#)]. The anatase phase, which is the most photoactive phase of titania, is present in the sample and ensures sufficient photocatalytic activity.

STEM-EDX measurements were performed on the powder sample to show the presence of silver. [Figure 3](#) shows a STEM image of its surface as well as silver and titanium mapping. Ag and Ti are both homogeneously dispersed on the surface ([Figure 3\(b,c\)](#)). Silver is a well-known additive in TiO_2 materials as it increases their

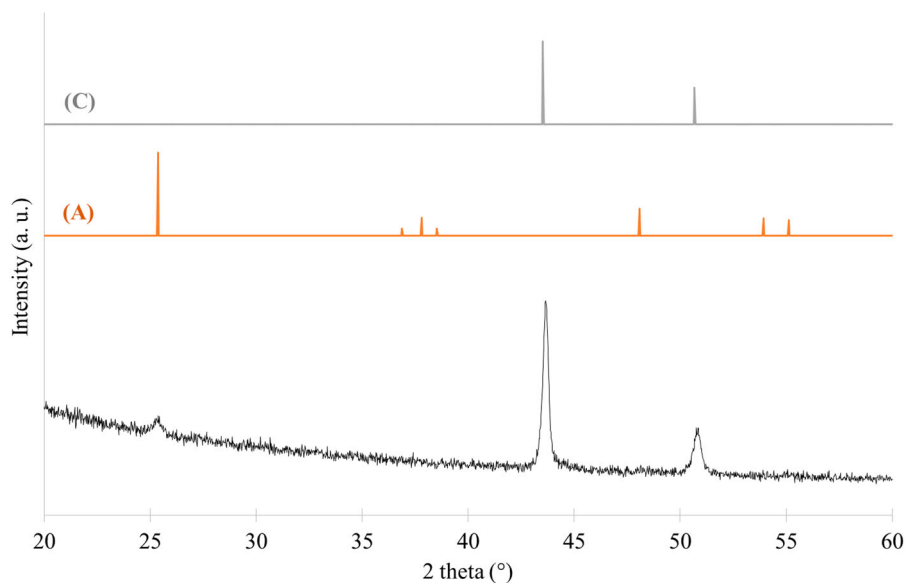


Figure 2. Grazing incident X-ray diffraction (GIXRD) pattern of the laboratory TiO_2 coating on steel. (A) Reference pattern of anatase and (C) Reference pattern of chromium iron carbide.

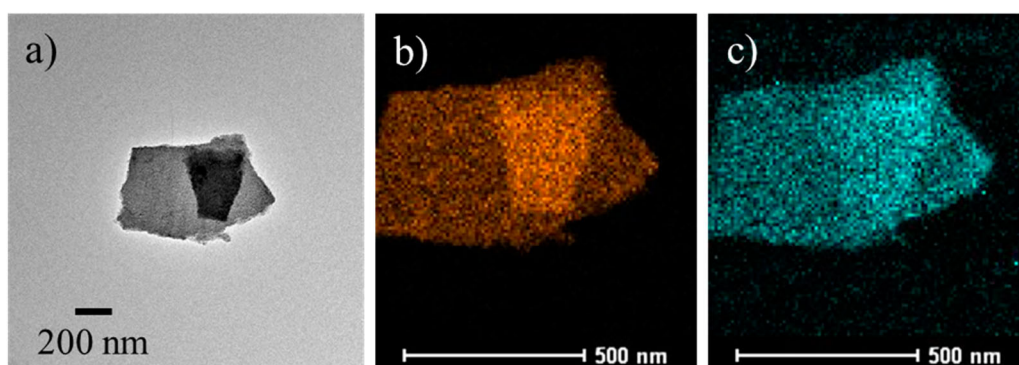


Figure 3. (a) STEM images of a particle of TiO_2 powder corresponding to the deposited layer, (b) Ag mapping and (c) Ti mapping.

photoefficiency by electron trapping [25,28]. The SEM-EDX measurement of the coating on steel is presented in Supplementary Materials (Figure S1). The presence of silver at the surface is made less obvious by the high noise caused by the support's iron and chromium.

3.1.2. Degradation tests

The degradation efficiency of the combined ozonation-photocatalytic process was evaluated at laboratory scale on the laboratory-made water containing 22 micropollutants. The results are presented in Table 3. These substances were chosen because they are listed in the WFD [29–31] of the European Commission as priority substances found at the exit of a WWTP.

The limit of detection is $0.4 \mu\text{g/L}$ for the GC-MS/MS method (first half of the micropollutants list in Table 3) and $0.025 \mu\text{g/L}$ for the LC-MS/MS method (second half of the micropollutants list in Table 3). The error,

therefore, is around 5% for the GC-MS/MS method and 1% for the LC-MS-MS method.

Only the concentrations of the initial molecules are followed, and the measured degradation does not necessarily correspond to a mineralization.

The results show that 8 substances are completely removed and 5 partially eliminated after the ozonation step. With the use of UVC light, 9 pollutants partially or fully resistant to ozonation are now completely eliminated. Two more compounds are also partially eliminated. With the use of TiO_2 photocatalysis, 6 molecules resistant or partially resistant to the previous processes now experience a higher degradation.

As described before, an additional step of GAC adsorption is used at pre-industrial scale in order to adsorb residual pollutants and transformation products from the ozonation and the UVC photocatalysis

Table 3. Degradation efficiencies in absolute percentage on the model polluted water for the sprayed sample at laboratory scale.

Pollutant	Degradation with O_3 (%)	Degradation with UVC (%)	Degradation with UVC - photocatalysis (%)	Total degradation (%)
Lindane	0	0	18	18
Atrazine	0	100	–	100
Brominated diphenyl ether	0	100	–	100
Tributylphosphate	0	0	62	62
Di(2-ethylhexyl)phthalate	0	9	74	83
Metoprolol	50	11	39	100
Carbamazepine	100	–	–	100
Diclofenac	100	–	–	100
Sulfamethoxazole	100	–	–	100
1H-benzotriazole	0	84	10	94
Desethylatrazine	0	100	–	100
2,6-dichlorobenzamide	0	0	32	32
Bromacile	85	15	–	100
Simazine	100	–	–	100
Chlortoluron	100	–	–	100
Isoproturon	100	–	–	100
DDT	9	91	–	100
Acetyl-4-Sulfamethoxazole	43	57	–	100
Iohexole	6	94	–	100
Iopromide	0	100	–	100
Clarithromycin	100	–	–	100
Terbutryn	100	–	–	100

–: already eliminated before this treatment.

treatments. In the next section, the different GAC will be tested to select an efficient adsorbent on the target micropollutants.

3.1.3. Adsorption experiments

As observed in Table 3, some micropollutants were not fully degraded after the combined ozonation-UVC photocatalysis treatment: an adsorption step will be necessary to purify the water completely.

Two resistant micropollutants largely present in Germany were selected for the adsorption experiments: metoprolol and 1H-benzotriazole. Seven commercial

carbon materials were chosen; the list is denoted in Table 1.

Each carbon sample (2 mg) was mixed with 200 mL of a solution of 10 µg/L of both micropollutants; their concentrations were followed for 120 min. The evolution of the concentration is represented on Figure 4(a) for metoprolol and 4b for 1H-benzotriazole.

For all carbon materials, similar shapes were observed when analyzing the curves in Figure 4, corresponding to a quick adsorption in the first 30 min, then a slower adsorption. Five carbon materials presented higher adsorption rates for both compounds: DC CX30, DC A,

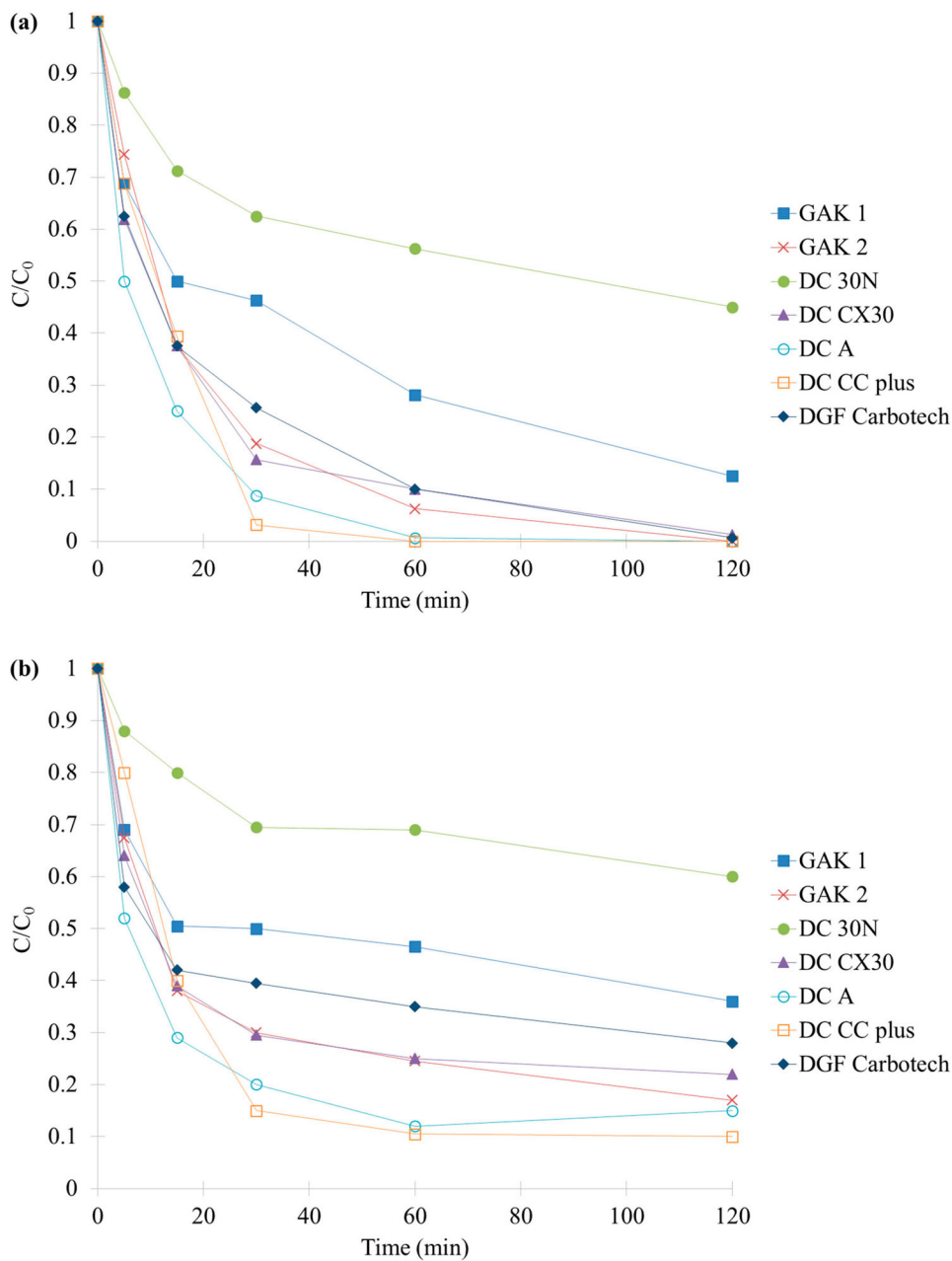


Figure 4. Evolution of the concentration of (a) metoprolol and (b) 1H-benzotriazole with the different carbon materials.

DC CC plus and DGF Carbotech. The best one was DC CC plus.

In order to refine the selection of the carbon material for a large scale application, two other criteria were explored: the specific surface area and the cost of the materials. Both parameters are reported in Table 1. The specific surface area, S_{BET} , is related to the available surface of the material to adsorb pollutant and the cost is obviously an important criterion for industrial applications.

Concerning the price, DC 30N and DGF Carbotech materials have the lowest price (1880 and 1410 €/ton, respectively). They both have a similar specific surface area (around 1000–1050 m²/g), but DGF Carbotech presented better adsorption properties on both micropollutants (Figure 4(a,b)). DC A and DC CC plus showed the highest S_{BET} values and also the best adsorption properties, but they were quite expensive (2700 and 3895 €/ton, respectively). GAK 1, GAK 2 and DC CX30 had intermediate price (~ 2300 €/ton) and specific surface area around 950 m²/g.

Following the three criteria, the selected carbon was DGF Carbotech material. It represented the best compromise between adsorption properties and price.

3.2. Pilot scale

The TiO₂ coating developed at laboratory scale has been successfully deposited inside the steel pilot reactor [5]. This reactor has been tested for the treatment of four different compositions of polluted waters: one laboratory-made water, two industrial waters and one municipal water.

Table 5. Toxicity tests at pilot scale with the different polluted waters.

	Toxicity parameters	Before ozone	After ozone (30 min)	After ozone (30 min) and photocatalysis (1 h)
Model water	EC50 (%)	12.5	61.5	83
	TU	8	1.6	1.2
Textile water	EC50 (%)	0.25	2.8	0.9
	TU	400	35	110
Culture media	EC50 (%)	2.5	28.8	29.3
	TU	40	3.5	3.4
Municipal water	EC50 (%)	>100	>100	>100
	TU	0	0	0

EC50: the effluent relative concentration at which half of the microorganisms (*Daphnia Magma*) are dead; TU: 100%/EC50 is an indicator for toxicity; the water is considered as toxic if TU > 1, and very toxic if TU > 10.

The results for the treatment of the laboratory-made water are shown in Table 4. Similar results compared to laboratory scale were obtained: 16 out of 22 micropollutants were completely degraded after the ozonation and UVC steps and 6 molecules were still present after both treatments. Photocatalysis improved the degradation of all these molecules. This experiment showed the successful scaling-up of the combined ozonation-UVC photocatalytic process.

Concerning the experiments on industrial waters, Table 5 shows the evolution of the water toxicity before the treatment, after the ozonation step and after the combined process. Water originating from the chosen textile industry is highly toxic (TU = 400; water is considered very toxic if TU > 10). After the treatment, only a low decrease of toxicity was observed with or without coating. In this case, it was assumed that biocides used for disinfection in the textile industry are

Table 4. Evaluation of the degradation efficiency at pilot scale after 30 min of ozonation and after a further 1 h of photocatalysis.

Pollutant	Degradation with O ₃ (%)	Degradation with UVC (%)	Degradation with UVC – photocatalysis (%)	Total degradation (%)
Lindane	0	0	22	22
Atrazine	0	100	–	100
Tributylphosphate	0	5	38	43
Di(2-ethylhexyl)phthalate	0	0	25	25
Desethylatrazine	0	100	–	100
2,6-dichlorobenzamide	0	0	20	20
Bromacile	100	–	–	100
Simazine	90	–	10	100
Chlortoluron	100	–	–	100
Isoproturon	100	–	–	100
DDT	17	83	–	100
Metoprolol	100	–	–	100
Carbamazepine	100	–	–	100
Diclofenac	100	–	–	100
Sulfamethoxazole	100	–	–	100
1H-benzotriazole	0	92	5	97
Acetyl-4-Sulfamethoxazole	40	60	–	100
Iohexole	–	100	–	100
Iopromide	–	100	–	100
Clarithromycin	100	–	–	100
Terbutryn	100	–	–	100
Brominated diphenyl ether	100	–	–	100

The adsorption contribution is subtracted from the results. The values correspond to the degradation attributable to a given process.

Table 6. Detected micropollutants in the municipal water and the evolution of their concentration with the pilot scale process.

Micropollutants detected	Concentration detected (ng/L)	Concentration after 30 min ozonation (ng/L)	Concentration after 30 min ozonation + 1 h UVC (ng/L)	Concentration after 30 min ozonation + 1 h UVC with photocatalyst (ng/L)
1H-benzotriazole	970	49	39	40
Carbamazepine	400	<	<	<
Clarithromycin	210	<	<	<
Diclofenac	840	<	<	<
Metoprolol	98	<	<	<
Sulfamethoxazole	2900	<	<	<
Terbutryn	52	<	<	<
Acetyl-4-Sulfamethoxazole	<	<	<	<
Iohexole	110,000	30,000	95	<
Iopromide	12,000	3300	<	<

<: inferior to the limit of detection (mentioned in supplementary materials).

not sensitive to ozonation and photocatalysis, or that at least a longer treatment time would be required. One of the insights that can be drawn from the experiment is that the efficiency of an advanced oxidation process depends on the water composition. Moreover, very high concentrations are not suitable for ozonation and UVC-based processes, let alone for photocatalysis. As a consequence, this type of water must always go through the first and secondary treatments of the waste water plant before undergoing the AOP, or another technique must be used to decrease significantly the concentration of the pollutants. With this cleaning textile wastewater, adsorption tests were performed on granular activated carbon and it was shown that the toxicity after adsorption decreases to TU = 40.

Water from the industry producing culture media was also highly toxic when it was received. This time, a significant decrease of toxicity after the AOP was shown in Table 5. The efficiency of the AOP on this type of water can be attributed to the overall lower concentrations of pollutants, as well as their type (organic pollutants).

Finally, the pilot was tested with municipal waste water. Water at the exit of the WWTP was collected in Esneux (Belgium) because of its proximity to a hospital. Toxicity before and after treatment was characterized

thanks to the *Daphnia Magna* test. As expected at the outlet of a WWTP, the water is considered not toxic (Table 5). Nevertheless, we know from LC-MS/MS analyses that some micropollutants are present, including most of those that we had targeted in the previous sections. Their concentrations range from a few ng/L (terbutryn) to 110 µg/L (Iohexol). The concentrations of these micropollutants were measured before and after the treatment (Table 6). Of 11 substances, 8 were fully eliminated by ozone only. Iopromide was removed by ozone and UVC light. Elimination of Iohexol is improved thanks to the photocatalytic coating.

3.3. Pre-industrial scale

Scaling-up was done successfully and water from the Duisburg WWTP was tested continuously for degradation. Corresponding results are presented in Table 7. Some water parameters followed, during the experiments, are also listed in Table 8.

When only ozonation and UVC light are used, with no photocatalysis, the flow rate must be low to obtain high degradations. For example, diclofenac degradation falls from 73% to 31% when increasing the flow rate from 1.6 m³/h to 4.6 m³/h; the same conclusion can be

Table 7. Evaluation of the degradation efficiency at pre-industrial scale after one pass through (some of) the treatments (ozonation, UVC/photocatalysis, adsorption).

Pollutant	Degradation (%) in the following conditions				
	FR = 4.6 m ³ /h LI = 23 W/m ² No coating (conditions 1)	FR = 4.6 m ³ /h LI = 33 W/m ² With coating (conditions 2)	FR = 1.6 m ³ /h LI = 23 W/m ² No coating(conditions 3)	FR = 4.2 m ³ /h LI = 350 W/m ² No coating (conditions 4)	FR = 4.6 m ³ /h LI = 23 W/m ² No coating After adsorption(conditions 5)
1H-benzotriazole	0	12	20	97	98
Carbamazepine	0	0	4	38	100
Clarithromycin	11	15	0	29	92
Diclofenac	31	48	73	100	100
Metoprolol	2	0	6	42	100
Sulfamethoxazole	7	12	37	87	100
Iohexole	29	6	92	94	95
Iopromide	12	18	69	87	100

FR: flow rate; LI: light intensity.

Table 8. Evolution of characteristic waste water parameters treated in the pre-industrial reactor during the different experiments described in Table 7.

Conditions of the trials (from Table 7)	DOC (mg/L)	pH	Turbidity ₂₅₄ (m ⁻¹)	COD (mg O ₂ /L)	Conductivity (μS/cm)
Conditions 1					
• Before O ₃	6.4	6.80	16.5	16.9	770
• After O ₃	6.6	6.88	13.5	15.5	767
• After UV	6.3	6.91	11.9	9.0	768
Conditions 2					
• Before O ₃	6.9	6.92	16.3	14.8	768
• After O ₃	6.4	6.89	12.0	14.8	770
• After UV	6.3	6.87	10.9	14.7	769
Conditions 3					
• Before O ₃	5.1	6.89	13.3	2380	532
• After O ₃	4.9	7.01	10.0	1766	541
• After UV	4.7	6.96	8.4	1750	539
Conditions 4					
• Before O ₃	6.0	6.80	15.2	14.7	769
• After O ₃	6.4	6.84	10.1	14.9	766
• After UV	6.4	6.88	9.5	13.8	767
Conditions 5					
• Before O ₃	7.4	6.83	- ^a	- ^a	21.5
• After O ₃	7.4	6.87	- ^a	- ^a	20.4
• After UV	7.4	6.73	- ^a	- ^a	20.3
• After adsorption	0.4	6.41	- ^a	- ^a	30.9

DOC: dissolved organic carbon; COD: chemical oxygen demand; Turbidity₂₅₄: UV absorption coefficient at 254 nm; -^a: not measured.

drawn for sulfamethoxazole, iohexole and iopromide. The flow rate is thus an important parameter which can help control the desired concentration at the outlet of the AOP.

Using a coated reactor, one can degrade pollutants that would not have been degraded otherwise. In this series of experiments, it is the case of 1H-benzotriazole. Previous experiments and previous works have shown that other micropollutants fall into this category. Efficiency of photocatalysis is lower in the pre-industrial experiment than other AOPs, because of the lower surface of photocatalyst to volume of water ratio. However, the process still benefits from this addition, as shown by increases in the degradation of diclofenac and iopromide.

As expected, increasing the light intensity more than tenfold sharply improves the results. However, it also increases the energy consumption proportionally and

decreases the relative efficiency of the photocatalysis process (as mass transfer becomes rate-determining at high light intensities). While increasing the light intensity is an efficient solution, it is also more expensive.

Finally, adsorption is very efficient at eliminating all molecules almost fully. The drawback of using adsorbents is that they need to be replaced regularly, interrupting the continuous process. Nevertheless, when it is possible, two adsorption columns can be placed: one operating when the other is regenerated. In this case, it increases the cost of the installation.

Concerning the water parameters (Table 8), the dissolved organic carbon (DOC), the chemical oxygen demand (COD) and the turbidity (Turbidity₂₅₄) decreased during the global process. These parameters are clearly linked to the amount of organic pollutants; it is, therefore, logical that their values decreased when the micropollutants are degraded. pH and conductivity of the water in these processes are mostly constant ($\Delta\text{pH}_{\text{max}}$ of 0.4 and $\Delta\text{Conductivity}_{\text{max}}$ of 9 $\mu\text{S}/\text{cm}$).

4. Conclusions

In our previous work, a global advanced oxidation process was developed to degrade environmentally harmful organic micropollutants in waste water, using ozonation, UVC light and photocatalysis. This present work corresponds to our previous results scaled up to pre-industrial scale (around 5 m³/h).

In the first part of this work, the optimized syntheses are tested at laboratory scale. The anatase layers are proved to be efficient for the degradation of most micropollutants. Furthermore, different adsorbent carbon materials are tested, so that a compromise between the efficiency and the price can be made with scaling up in mind.

In the second part, the scale is increased to pilot scale, using both laboratory-made waters and industrial waters. The toxicity of the water is controlled in every case, as well as the micropollutant concentration. It is found that the efficiency of the different steps (ozonation, UV, photocatalysis) depends strongly on the type of water treated. In particular, photocatalysis is more efficient for low-toxicity waters and ozonation and UVC should be used when the water is more toxic.

In the last part of the study, pre-industrial tests were conducted as a tertiary treatment for waste water. It is shown that the main parameters for the efficiency of the process are the flow rate and the light intensity. The photocatalyst plays a role by degrading more persistent micropollutants. Adsorption, in this case, is very efficient, with an overall elimination >95% of all substances investigated. The AOPs help extend the lifetime of the adsorbent.

The results show that combining advanced oxidative processes is an efficient solution at large scale, especially when it is used synergistically with adsorption.

Acknowledgements

S. D. L. and S. H. thank the Belgian National Funds for Scientific Research (F.R.S.-FNRS) for their Senior Associate Researcher and Research Director position respectively. For their financial support, the authors are grateful to the Ministère de la Région Wallonne Direction Générale des Technologies, de la Recherche et de l'Énergie (DGO6), in relation to the Plan Marshall, and with support from the '22nd CORNET Call' funds for the research project 'AOPTi - Advanced photocatalytic oxidation processes for micropollutant elimination in municipal and industrial water'. The authors also would like to thank for the financial support from the German Federal Ministry of Economic Affairs and Energy within the agenda for the promotion of industrial cooperative research and development (IGF) in relation to the CORNET programme based on the decision of the German Bundestag. The access was opened by member organization environmental technology and organized by the AiF, Arbeitsgemeinschaft industrieller Forschungsvereinigungen, Cologne (IGF-Project No. 202 EN). The authors thank Aquatic Science S.A. for the use of the spray coating equipment. The authors also thank the CAREM platform and Ir. Artium Belet of the University of Liège for SEM-STEM measurements.

Disclosure statement

No potential conflict of interest was reported by the author(s).

Funding

This work was supported by 22nd CORNET Call; German Federal Ministry of Economic Affairs and Energy.

Data availability statement

The raw/processed data required to reproduce these findings cannot be shared at this time as the data also form part of an ongoing study.

ORCID

Julien G. Mahy  <http://orcid.org/0000-0003-2281-9626>
Sophie Hermans  <http://orcid.org/0000-0003-4715-7964>

References

- [1] Khan MA, Ghouri AM. Environmental pollution: its effects on life and its remedies. *J Arts Sci Commer.* 2011;2:276–285.
- [2] Belet A, Wolfs C, Mahy JG, et al. Sol-gel syntheses of photocatalysts for the removal of pharmaceutical products in water. *Nanomaterials.* 2019;9:126. DOI:10.3390/nano9010126.
- [3] Luo Y, Guo W, Ngo HH, et al. A review on the occurrence of micropollutants in the aquatic environment and their fate and removal during wastewater treatment. *Sci Total Environ.* 2014;473–474:619–641. DOI:10.1016/j.scitotenv.2013.12.065.
- [4] Lapworth DJ, Baran N, Stuart ME, et al. Emerging organic contaminants in groundwater: a review of sources, fate and occurrence. *Environ Pollut.* 2012;163:287–303. DOI:10.1016/j.envpol.2011.12.034.
- [5] Mahy JG, Wolfs C, Mertes A, et al. Advanced photocatalytic oxidation processes for micropollutant elimination from municipal and industrial water. *J Environ Manage.* 2019;250:109561. DOI:10.1016/j.jenvman.2019.109561.
- [6] Vatankhah H, Riley SM, Murray C, et al. Simultaneous ozone and granular activated carbon for advanced treatment of micropollutants in municipal wastewater effluent. *Chemosphere.* 2019;234:845–854. DOI:10.1016/j.chemosphere.2019.06.082.
- [7] Ma XY, Wang Y, Dong K, et al. The treatability of trace organic pollutants in WWTP effluent and associated biotoxicity reduction by advanced treatment processes for effluent quality improvement. *Water Res.* 2019;159:423–433. DOI:10.1016/j.watres.2019.05.011.
- [8] da Silva L, Jardim WF. Trends and strategies of ozone application in environmental problems. *Quim Nova.* 2006;29:310–317.
- [9] Mahy JG, Deschamps F, Collard V, et al. Acid acting as redispersing agent to form stable colloids from photoactive crystalline aqueous sol-gel TiO₂ powder. *J Sol-Gel Sci Technol.* 2018;87:568–583. DOI:10.1007/s10971-018-4751-6.
- [10] Mahy JG, Paez CA, Carcel C, et al. Porphyrin-based hybrid silica-titania as a visible-light photocatalyst. *J Photochem Photobiol A Chem.* 2019;373:66–76. DOI:10.1016/j.jphotochem.2019.01.001.
- [11] Pelaez M, Nolan NT, Pillai SC, et al. A review on the visible light active titanium dioxide photocatalysts for environmental applications. *Appl Catal B Environ.* 2012;125:331–349. DOI:10.1016/j.apcatb.2012.05.036.
- [12] Pignatello JJ, Oliveros E, MacKay A. Advanced oxidation processes for organic contaminant destruction based on the fenton reaction and related chemistry. *Crit Rev Environ Sci Technol.* 2006;36:1–84. DOI:10.1080/10643380500326564.
- [13] Villegas-Guzman P, Giannakis S, Rtimi S, et al. A green solar photo-Fenton process for the elimination of bacteria and micropollutants in municipal wastewater treatment using mineral iron and natural organic acids. *Appl Catal B Environ.* 2017;219:538–549. DOI:10.1016/j.apcatb.2017.07.066.
- [14] López-Vinent N, Cruz-Alcalde A, Romero LE, et al. Synergies, radiation and kinetics in photo-Fenton process with UVA-LEDs. *J Hazard Mater.* 2019;380:120882. DOI:10.1016/j.jhazmat.2019.120882.
- [15] Yang L, Bai X, Shi J, et al. Quasi-full-visible-light absorption by D35-TiO₂/g-C₃N₄ for synergistic persulfate activation towards efficient photodegradation of micropollutants. *Appl Catal B Environ.* 2019;256; DOI:10.1016/j.apcatb.2019.117759.
- [16] Wardenier N, Liu Z, Nikiforov A, et al. Micropollutant elimination by O₃, UV and plasma-based AOPs: an evaluation of treatment and energy costs. *Chemosphere.* 2019;234:715–724. DOI:10.1016/j.chemosphere.2019.06.033.

- [17] Seo C, Shin J, Lee M, et al. Elimination efficiency of organic UV filters during ozonation and UV/H₂O₂ treatment of drinking water and wastewater effluent. *Chemosphere*. 2019;230:248–257. DOI:10.1016/j.chemosphere.2019.05.028.
- [18] Miklos DB, Remy C, Jekel M, et al. Evaluation of advanced oxidation processes for water and wastewater treatment – A critical review. *Water Res*. 2018;139:118–131. DOI:10.1016/j.watres.2018.03.042.
- [19] Donau carbon prices. n.d.. [cited 2019 Jan 28]. Available from: https://donau-carbon.com/Products-Solutions/Aktivkohle/Produktubersicht/Hydraffin*?lang=en-US.
- [20] CSC carbon prices. n.d. [cited 2019 Jan 28]. Available from: https://www.carbon-service.de/swimming_pool_water.htm.
- [21] Carbotech prices. n.d. [cited 2019 Jan 28]. Available from: <https://www.carbotech.de/aktivkohle/?lang=en>.
- [22] Lecloux AJ. Texture of catalysts. *Catal Sci Technol*. 1981;2:171.
- [23] [ISO] International Standard. Water quality – determination of the inhibition of the mobility of *Daphnia magna* Straus (Cladocera, Crustacea) – acute toxicity test, Int. Stand. ISO 6341, 2012.
- [24] Léonard GL-M, Malengreaux CM, Mélotte Q, et al. Doped sol–gel films vs. powders TiO₂: On the positive effect induced by the presence of a substrate. *J Environ Chem Eng*. 2016;4:449–459. DOI:10.1016/j.jece.2015.11.040.
- [25] Bodson CJ, Heinrichs B, Tasseroul L, et al. Efficient P- and Ag-doped titania for the photocatalytic degradation of waste water organic pollutants. *J Alloys Compd*. 2016;682:144–153. DOI:10.1016/j.jallcom.2016.04.295.
- [26] Ohtani B, Prieto-Mahaney OO, Li D, et al. What is Degussa (Evonic) P25? Crystalline composition analysis, reconstruction from isolated pure particles and photocatalytic activity test. *J Photochem Photobiol A Chem*. 2010;216:179–182. DOI:10.1016/j.jphotochem.2010.07.024.
- [27] Mahy JG, Lambert SD, Tilkin RG, et al. Ambient temperature ZrO₂-doped TiO₂ crystalline photocatalysts: highly efficient powders and films for water depollution. *Mater Today Energy*. 2019;13:312–322. DOI:10.1016/j.mtener.2019.06.010.
- [28] Espino-estévez MR, Fernández-rodríguez C, González-díaz OM. Effect of TiO₂ – Pd and TiO₂ – Ag on the photocatalytic oxidation of diclofenac, isoproturon and phenol. *Chem Eng J*. 2016;298:82–95. DOI:10.1016/j.cej.2016.04.016.
- [29] E. Commission. Water framework directive implementation reports, 2015. [cited 2019 March 25]. Available from: http://ec.europa.eu/environment/water/water-framework/impl_reports.htm.
- [30] Directive 2013/39/EU of the European Parliament, 2013. [cited 2019 Aug 1]. Available from: <https://eur-lex.europa.eu/legal-content/EN/ALL/?uri=CELEX%3A32013L0039>.
- [31] Commission Implementing Decision (EU) 2018/840, 2018. [cited 2019 August 1]. Available from: <https://eur-lex.europa.eu/legal-content/EN/TXT/?uri=CELEX%3A32018D0840>